

Supporting Information

Supplementary Figure Legends

Fig.S1. Impact of CR on NAD(P)H decay kinetics in the mouse dentate gyrus.

Distributions of the mean fluorescence lifetime τ_m (top row), the short component τ_1 corresponding to free NAD(P)H (upper middle row), long component τ_2 corresponding to bound NAD(P)H (lower middle row), and a_1 , the relative contribution of τ_1 to τ_m (bottom row) are shown by (A) region and (B) diet for the granular layer (GL), polymorphic layer (PL), molecular layer (ML) from 20-month-old Control (n=6) and CR (n=6) mice, ($_{\text{ex}}\lambda_{780}\text{nm}$).

Fig.S2. Impact of caloric restriction on expression of cytochrome c oxidase activity, succinate dehydrogenase activity, AMPK, and pAMPK in mouse hippocampus. (A) Quantification of cytochrome C oxidase stain intensity in the CA3 Cell Bodies (CA3CB) and CA3 Neuropil (CA3NP) from Control (n=3) and CR mice (n=3). (B) Quantification of succinate dehydrogenase stain intensity in the CA3 Cell Bodies (CA3CB) and CA3 Neuropil (CA3NP) from Control (n=5) and CR mice (n=5). (C) pAMPK stain intensity within the whole hippocampus (WH), granular layer (GL), polymorphic layer (PL), molecular layer (ML), CA3 Cell Bodies (CA3CB), and CA3 Neuropil (CA3NP) from Control (n=5) and CR mice (n=5). (D) pAMPK stain intensity within the whole hippocampus (WH), granular layer (GL), polymorphic layer (PL), molecular layer (ML), CA3 Cell Bodies (CA3CB), and CA3 Neuropil (CA3NP) from Control (n=3) and CR mice (n=3). (E) Representative images of AMPK immunodetection in the dentate gyrus from a Control mouse (grayscale and inverted). Data shown as average \pm SEM (*p<0.05)

Fig.S3 Impact of caloric restriction on expression of PGC-1 α and GSK3 β in mouse hippocampus. (A) Quantification of PGC-1 α stain intensity in the CA3 Cell Bodies (CA3CB) and CA3 Neuropil (CA3NP) from Control (n=3) and CR mice (n=3). (B) Quantification of GSK3 β stain intensity in the CA3 Cell Bodies (CA3CB) and CA3 Neuropil (CA3NP) from Control (n=4) and CR mice (n=5). Data shown as average \pm SEM (*p<0.05)

Fig.S4 Impact of caloric restriction on expression of pGSK3 β in mouse hippocampus. (A) Quantification of pGSK3 β stain intensity within the whole hippocampus (WH), granular layer (GL), polymorphic layer (PL), molecular layer (ML), CA3 Cell Bodies (CA3CB), and CA3 Neuropil (CA3NP) from Control (n=4) and CR mice (n=5). (B) Representative image of pGSK3 β immunodetection in the dentate gyrus from a Control mouse (grayscale and inverted). (C) Quantification of pGSK3 β /total GSK3 β ratio within the whole hippocampus (WH), granular layer (GL), polymorphic layer (PL), molecular layer (ML), CA3 Cell Bodies (CA3CB), and CA3 Neuropil (CA3NP) from Control (n=4) and CR mice (n=5). Data shown as average \pm SEM (*p<0.05). CR x Region* indicates significant interaction.

Fig.S5. Representative image of immunodetection of hippocampal PGC-1 α in an 18-year-old rhesus monkey. PGC-1 α is detected throughout the hippocampus.

Fig.S6. Impact of caloric restriction on expression of PGC-1 α , GSK3 β , and pGSK3 β in rhesus monkey hippocampus. (A) Quantification of PGC-1 α stain intensity in the CA3 Cell Bodies (CA3CB) and CA3 Neuropil (CA3NP) Control (n=7) and CR (n=6) monkeys. (B) Quantification of GSK3 β stain intensity in the CA3 Cell Bodies (CA3CB) and CA3 Neuropil (CA3NP) Control (n=7) and CR (n=6) monkeys. (C) Quantification of pGSK3 β

stain intensity within the whole hippocampus (WH), granular layer (GL), polymorphic layer (PL), molecular layer (ML), CA3 Cell Bodies (CA3CB), and CA3 Neuropil (CA3NP) from Control (n=7) and CR (n=6) monkeys. (D) Quantification of pGSK3 β /GSK3 β in the CA3 Cell Bodies (CA3CB) and CA3 Neuropil (CA3NP) Control (n=7) and CR (n=6) monkeys. Data shown as average \pm SEM (*p<0.05)

Figure S1

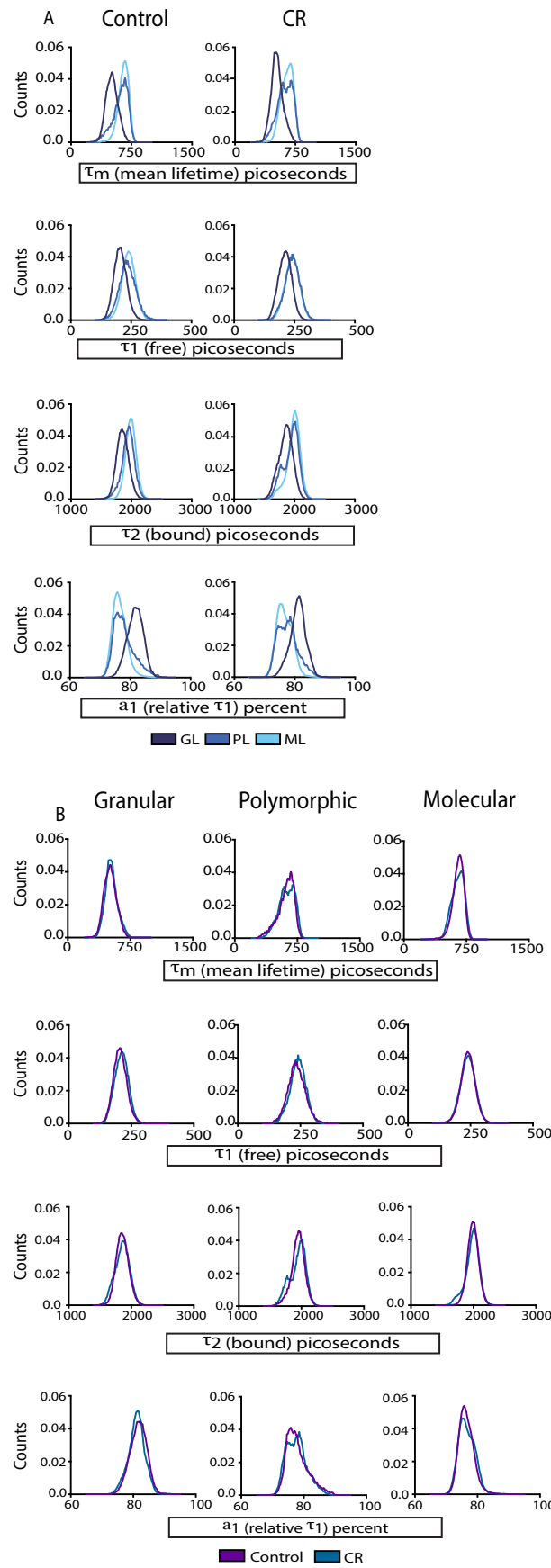


Figure S2

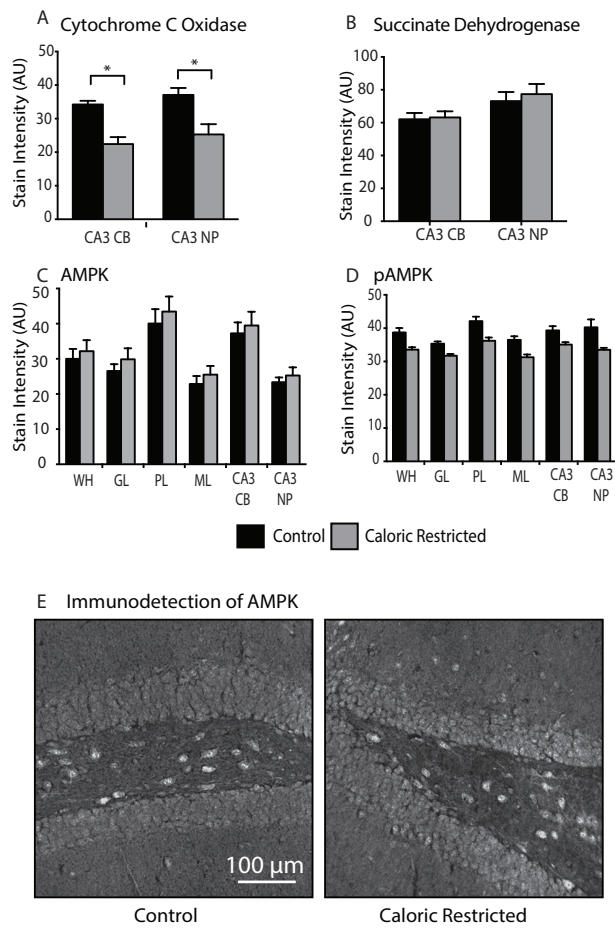


Figure S3

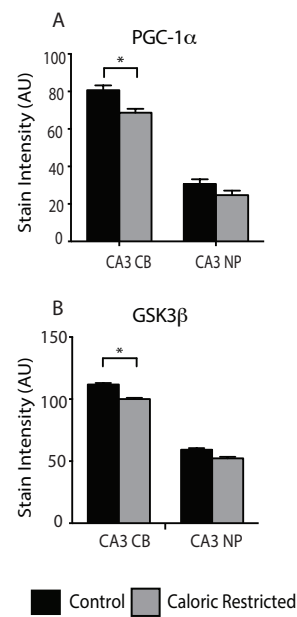


Figure S4

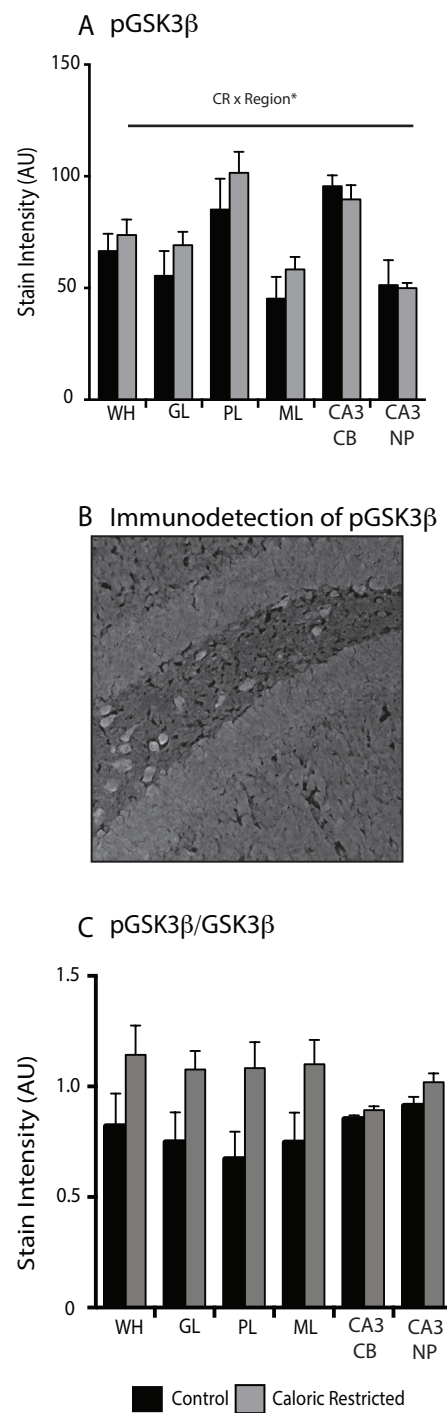


Figure S5

Immunodetection of PGC-1 α



Whole Hippocampus (Monkey)

Figure S6

